Talanta 85 (2011) 1798–1804

Contents lists available at ScienceDirect

Talanta

journal homepage: www.elsevier.com/locate/talanta

# Protonation and ion exchange equilibria of weak base anion-exchange resins

Yoshinobu Miyazaki*, Mariko Nakai

*Department of Chemistry, Fukuoka University of Education, Akamabunkyo-machi, Munakata, Fukuoka 811-4192, Japan*

ARTICLE INFO

*Article history:*
Received 16 May 2011
Received in revised form 6 July 2011
Accepted 6 July 2011
Available online 14 July 2011

*Keywords:*
Weak base anion-exchange resin
Acrylic resin
Protonation
Tertiary amine
NMR spectroscopy

ABSTRACT

Protonation and ion exchange equilibria of weak base anion-exchange resins, in which tertiary amine moieties were introduced as a functional group, were investigated by applying NMR spectroscopy to species adsorbed into the resins. $^{31}$P NMR signals of the phosphinate ion in the resin phases shifted to a lower field due to the influence of protonation of the tertiary amine groups of the resins in the pH range of 4–10. Protonation constants of the tertiary amine groups in styrene–divinylbenzene (DVB)-based resins were estimated to be $K_H = 10^{6.4}$ for Amberlite IRA96 and $10^{6.5}$ for DIAION WA30 by the $^{31}$P NMR method using the phosphinate ion as a probe species. In addition to the low field shift caused by the protonation of the tertiary amine moieties, another low field shift was observed for the phosphinate ion in acrylic acid–DVB-based resins at a rather high pH. This shift should be due to an unexpected deprotonation in the acrylic resin: a tautomerism accompanying the proton release from the amide form to the imide one in the functional group, thus, the resin could exhibit a cation exchange property at the high pH. Protonation constants of the tertiary amine moieties in the acrylic resins were estimated to be $10^{8.8}$ for DIAION WA10, $10^{9.0}$ for Amberlite IRA67 and $10^{9.3}$ for Bio-Rad AG 4-X4 on the basis of the Henderson–Hasselbalch equation using the resin phase pH estimated by the $^{133}$Cs and $^{1}$H NMR signal intensities.



## 1. Introduction

Ion-exchange resins have been used in many fields such as water treatment, natural resource recoveries, hydrometallurgy, sugar manufacturing, food processing, pharmacy and medicine [1]. The resins have also been commonly used in the laboratory for the separation and concentration of minor species as a pretreatment of chemical quantification [2]. Various kinds of weak base anion-exchange resins are available as commercial ion-exchangers. They comprise a rather complex range of products, however, concrete information on their structures has not been well disclosed. There are two main matrices, *i.e.*, styrene–DVB and acrylic acid–DVB copolymers, which have fixed groups of primary, secondary and tertiary amine functionalities, individually or in mixtures. The resin internal phase can be regarded as a concentrated and heterogeneous crosslinked polyelectrolyte for the chemical reactivity of ions [3,4]. The ion exchange capacity and the selectivity depend on the degree of protonation of the functional group. The knowledge about protonation equilibria of the functional groups in such a special kind of solution would be important for their practical use as well as for understanding their ion exchange properties. A lot of effort has been devoted to work out for understanding and predicting the protonation, complexation and ion exchange equilibria of weak acid, weak base and chelating ion exchange resins [3,5,6]. One of the novel approaches is the Gibbs–Donnan model [7–9] to estimate protonation and complexation constants of the resins. Pesavento et al. successfully applied the Gibbs–Donnan model to describe and predict the ion exchange sorption through the estimation of the protonation and complexation constants, which were in good agreement with those of the monomeric models in aqueous solutions [10–13]. However, equilibria taking place inside resin phases have not been fully investigated yet, because there are few direct methods for probing the species adsorbed into such solid particle samples. NMR spectroscopy should be a promising and straightforward method for probing the species adsorbed into the experimentally and not easily accessible gel phase [14–19]. In our previous studies [20,21], the ion exchange selectivity of strong base anion-exchangers was studied by measuring the $^{31}$P NMR spectra of phosponate and phenylphosphate ions adsorbed into the resins, and a well-defined correlation between the selectivity coefficients and the gel phase $^{31}$P NMR chemical shift was elucidated. Recently, we also clarified the ion exchange and protonation behaviors of an amphoteric ion-exchange resin, which has strong base and weak acid moieties in a single functional group fixed on the styrene–DVB matrix based on the information about the concentrations of various kinds of salts in the resin's internal phase estimated by the NMR method [22]. The present investigation was undertaken to elucidate the protonation and ion exchange properties of styrene–DVB based and acrylic acid–DVB based weak base anion-exchange resins, in which tertiary amine groups were introduced as a functional group.

* Corresponding author. Tel.: +81 940 351 379; fax: +81 940 351 711.
*E-mail address:* miyazaky@fukuoka-edu.ac.jp (Y. Miyazaki).

0039-9140/$ – see front matter © 2011 Elsevier B.V. All rights reserved.
doi:10.1016/j.talanta.2011.07.010

**Table 1**
Physicochemical characteristics of investigated weak base anion-exchange resins.

| | Amberlite IRA96 | DIAION WA30 | Amberlite IRA67 | DIAION WA10 | AG 4-X4 |
|---|---|---|---|---|---|
| Physical form | Tan opaque, spherical beads | Tan opaque, spherical beads | Transparent white, spherical beads | Transparent white, spherical beads | Yellow-white opaque, powder |
| Matrix | Styrene–DVB | Styrene–DVB | Acrylic acid–DVB | Acrylic acid–DVB | Acrylic acid–DVB |
| Functional groups | Tertiary amine | Tertiary amine | Tertiary amine | Tertiary amine | Tertiary amine |
| Structure | Macroporous | Macroporous | Gel | Gel | Macroporous |
| Capacity (equiv./L) | 1.25 | 1.5 | 1.6 | 1.2 | 0.8 |
| Particle size range (mm) | 0.55–0.75 | 0.4–0.6 | 0.50–0.75 | 0.4–0.6 | 0.075–0.15 |
| Moisture content (%) | 57–63 | 43–55 | 56–64 | 63–69 | 40–45 |

## 2. Experimental

### 2.1. Chemicals and resins

Styrene–DVB-based weak base anion-exchange resins, Amberlite IRA96 (Rohm and Haas Co.) and DIAION WA30 (Mitsubishi Chemical Co.), and acrylic acid–DVB-based resins, Amberlite IRA67, DIAION WA10, AG 4-X4 (Bio-Rad Laboratories) were used in this study. Their physicochemical characteristics are summarized in Table 1. The conditioning of the resins was performed by a column method: the resins were placed into a glass column, and washed with successive, 2 bed volumes of 1 mol dm$^{-3}$ HCl, 5 bed volumes of water, 2 bed volumes of 1 mol dm$^{-3}$ NaOH, and 5 bed volumes of water. The prepared resins were stored under an air-dried condition. All other reagents were of analytical reagent grade and used as received. All solutions were prepared using deionized water.

### 2.2. NMR measurements for resin samples

The $^{31}$P, $^{133}$Cs and $^{1}$H NMR spectra were recorded by a JEOL JNM-ECX400 spectrometer at 161.8 MHz, 52.4 MHz and 399.8 MHz, respectively. The field frequency lock was achieved with the deuterium resonance of $D_2O$ in a concentric capillary tube. A series of 0.1 mol dm$^{-3}$ $NaPH_2O_2$ solutions (20 cm$^3$) of different pHs were equilibrated with 0.3 g of the air-dried styrene–DVB-based or acrylic acid–DVB-based resins. The pH of the solutions was adjusted using a small amount of NaOH or HCl solution. After equilibration had been reached, the resins were loaded into NMR sample tubes together with small amounts of the equilibrium solutions, and the $^{31}$P NMR spectra for the resin beds were then measured in the same way as that for an ordinary solution sample [17–22]. Thus, the observed NMR spectra for the resin bed contained signals of species both in the resin phase and in the interstitial equilibrium solution. The signal assignment was made by comparing the spectra of the resin beds with those of the equilibrium solutions without the resins. For the acrylic acid–DVB-based resins, the $^{133}$Cs and $^{1}$H NMR spectra for the resins in equilibrium with a series of 0.1 mol dm$^{-3}$ CsCl solutions of different pHs were also measured. Chemical shifts were reported with respect to 85% $H_3PO_4$ for $^{31}$P and 0.1 mol dm$^{-3}$ CsCl for $^{133}$Cs as the external references. Overlapping signals were resolved into individual peaks by a Lorentzian curve-fitting method [23].

## 3. Results and discussion

### 3.1. Analysis of protonation equilibria of amines by $^{31}$P NMR method

The $^{31}$P NMR chemical shift of the phosphinate ion is sensitive to the concentrations of amines and quaternary ammonium salts; the signal moves to a higher field when the concentration increases [24]. The chemical shift is also sensitive to the protonation degree of the amine, thus the phosphinate ion, whose protonation constant is $K_H = 10^{1.3}$ [25], can be used as a probe species for the protonation equilibrium analysis of amines. Fig. 1 shows the pH dependence of the $^{31}$P chemical shifts for triethanolamine (TEA) solutions containing a small amount of sodium phosphinate. The phosphinate signal shifted to a lower field for a pH in the range of 6–10 due to the protonation of TEA. The chemical shift of the phosphinate ion in the TEA solution, $\delta_P$, and the protonation constant of TEA are given by the following equations:

$$\delta_P = \frac{[TEAH^+]\delta_P^{TEAH^+} + [TEA]\delta_P^{TEA}}{[TEAH^+] + [TEA]} = \frac{K_H[H^+]\delta_P^{TEAH^+} + \delta_P^{TEA}}{K_H[H^+] + 1} \quad (1)$$

$$K_H = \frac{[TEAH^+]}{[TEA] \cdot [H^+]} \quad (2)$$

where $\delta_P^{TEAH^+}$ and $\delta_P^{TEA}$ are the $^{31}$P chemical shifts of the phosphinate ions in the protonated and unprotonated TEA solutions, respectively. The protonation constant $K_H$ was estimated by a least-square-fitting of the pH dependent chemical shift data in Fig. 1 to Eq. (1) and was found to be $K_H = 10^{7.9\pm0.1}$, which agreed well with the reported value ($K_H = 10^{7.8}$ [26]). This NMR technique can also be applied to the equilibrium analysis of the protonation of weak base anion-exchange resins, into which the amine groups are introduced.

### 3.2. Styrene–DVB-based resins

Amberlite IRA96 and DIAION WA30, which are commercially available weak base anion-exchange resins, have tertiary amine moieties as a functional group fixed in the styrene–DVB matrix.

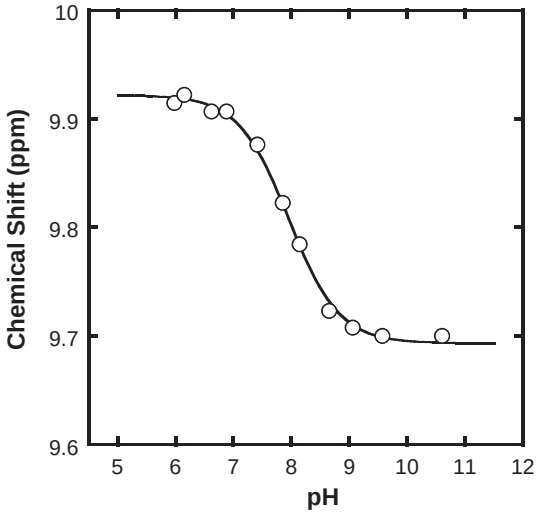


**Fig. 1.** The pH dependence of the $^{31}$P NMR chemical shifts for 1.2 mol dm$^{-3}$ TEA solutions containing 0.05 mol dm$^{-3}$ $NaPH_2O_2$.

The protonation equilibrium of the functional group and its thermodynamic protonation constant can be written as:

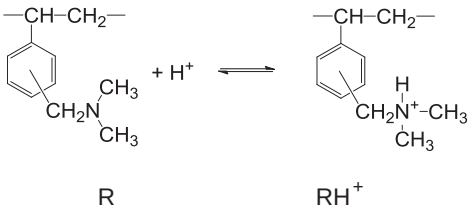

R RH$^+$ (3)

$$\bar{K}_H = \frac{\bar{a}_{RH^+}}{\bar{a}_R \cdot \bar{a}_H} = \frac{1-\alpha}{\alpha \cdot \bar{a}_H} \quad (4)$$

where the upper bar refers to the resin phase, and $a_X$ and $\alpha$ are the activity of the species $X$ and the degree of deprotonation, respectively. Since the activity of hydrogen ion in the resin phase cannot be directly measured, the apparent protonation constant, $\bar{K}_H^{app}$, where the activity of hydrogen ion in the resin phase is replaced with that in the equilibrium solution, has been conveniently used instead of the thermodynamic one [27–29].

$$\bar{K}_H^{app} = \frac{\bar{a}_{RH^+}}{\bar{a}_R \cdot a_H} = \frac{1-\alpha}{\alpha \cdot a_H} \quad (5)$$

The following equation can be obtained for the relation between $\log \bar{K}_H$ and $\log \bar{K}_H^{app}$ from Eqs. (4) and (5) using a Donnan equation [10,12,13,28]:

$$\log \bar{K}_H = \log \bar{K}_H^{app} + \log \frac{a_H}{\bar{a}_H} = \log \bar{K}_H^{app} + \log \frac{\bar{a}_A}{a_A} \quad (6)$$

where $A$ refers to a monovalent anion.

Fig. 2 shows the $^{31}$P NMR spectrum for Amberlite IRA96 in equilibrium with a 0.1 mol dm$^{-3}$ $NaPH_2O_2$ solution at pH 8.2. Two sets of triplet signals were observed; the higher field triplet signal was assigned to the phosphinate ion in the resin phase and the other to that in the interstitial equilibrium solution. It is obvious that the exchange rate of the phosphinate ion between the resin phase and the equilibrium solution was sufficiently slow on the NMR time-scale. The resin signal was broad and sometimes asymmetric

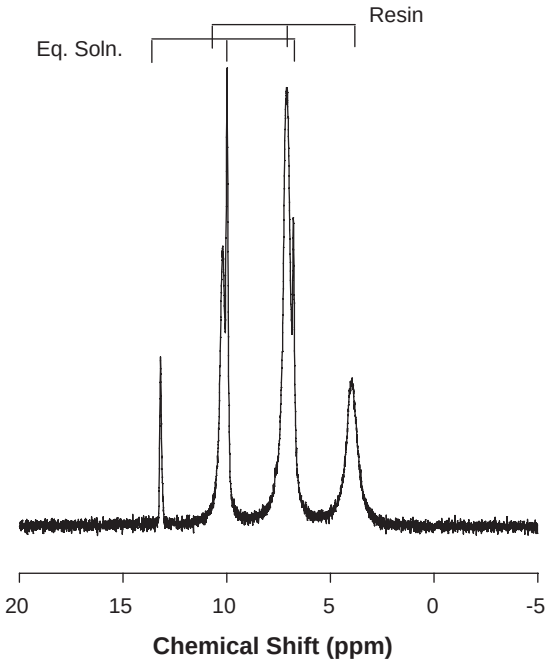


**Fig. 2.** The $^{31}$P NMR spectrum for the styrene–DVB-based weak base anion-exchange resin, Amberlite IRA96, in equilibrium with a 0.1 mol dm$^{-3}$ $NaPH_2O_2$ solution at pH 8.2.

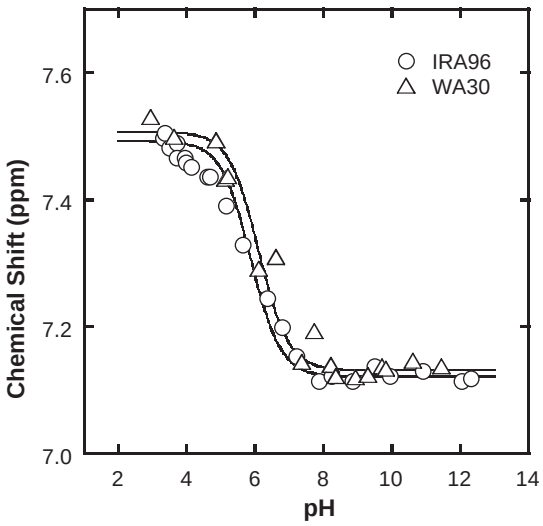


**Fig. 3.** The pH dependence of the $^{31}$P NMR chemical shifts of the phosphinate ion adsorbed into the styrene–DVB-based weak base anion-exchange resins.

reflecting the heterogeneity in the resin phase. The pH dependence of the $^{31}$P NMR chemical shifts of the phosphinate ion adsorbed into the styrene–DVB-based weak base anion-exchange resins is shown in Fig. 3. In the same way as that for TEA solution, the phosphinate signals for the resins shifted to a lower field at a lower pH in the range of 4–8 due to the protonation of the functional groups. The pH-dependent chemical shifts are given by the following equation:

$$\bar{\delta}_P = \frac{[\overline{RH^+}]\bar{\delta}_P^{RH^+} + [\bar{R}]\bar{\delta}_P^{R}}{[\overline{RH^+}] + [\bar{R}]} = (1-\alpha)\bar{\delta}_P^{RH^+} + \alpha\bar{\delta}_P^{R} \quad (7)$$

where $\bar{\delta}_P^{RH^+}$ and $\bar{\delta}_P^{R}$ are the $^{31}$P chemical shifts of the phosphinate ion in the protonated and unprotonated resins, respectively. These values were obtained from the limiting values of smooth curves fitted to the experimental points in Fig. 3 at low and high pHs; $\bar{\delta}_P^{RH^+}$ = 7.49 ppm and $\bar{\delta}_P^{R}$ = 7.12 ppm for IRA96, $\bar{\delta}_P^{RH^+}$ = 7.51 ppm and $\bar{\delta}_P^{R}$ = 7.13 ppm for WA30. Thus, the following equation is obtained from Eq. (7) to calculate the $\alpha$ values from the chemical shift data.

$$\alpha = \frac{\bar{\delta}_P - \bar{\delta}_P^{RH^+}}{\bar{\delta}_P^{R} - \bar{\delta}_P^{RH^+}} \quad (8)$$

We calculated the apparent protonation constants of the functional groups from the $^{31}$P NMR chemical shift data for the styrene–DVB-based resins. Fig. 4 shows the $\log \bar{K}_H^{app}$ *vs.* $\alpha$ plots for Amberlite IRA96 and DIAION WA30. The plot for DIAION WA30 shows some scatter due to the uncertainty of the chemical shifts caused by the resin phase heterogeneity. The $\log \bar{K}_H^{app}$ values increased with an increase in the degree of deprotonation. The resins have no fixed charge at $\alpha$ = 1 and the Donnan distribution term, $\log(\bar{a}_{PH_2O_2^-}/a_{PH_2O_2^-})$, can be assumed to be zero [27–29], which means that the hydrogen ion activities are the same between the resin phase and the equilibrium solution in Eq. (6). Therefore, the $\log \bar{K}_H^{app}$ value comes close to $\log \bar{K}_H$ when $\alpha$ approaches unity. Each $\log \bar{K}_H^{app}$ *vs.* $\alpha$ plot shown in Fig. 3 can be fitted to a straight line: $\log \bar{K}_H^{app} = (1.5 \pm 0.3)\alpha + (4.9 \pm 0.1)$ for IRA96; $\log \bar{K}_H^{app} = (0.5 \pm 0.5)\alpha + (6.0 \pm 0.3)$ for WA30. The $\log \bar{K}_H$ values were then estimated to be $6.4 \pm 0.4$ for Amberlite IRA96 and $6.5 \pm 0.8$ for DIAION WA30 by the extrapolation of the $\log \bar{K}_H^{app}$ values to $\alpha$ = 1.

In many cases the protonation and complexation inside the resins are related to the corresponding equilibria of the monomeric models in an aqueous solution [10–13]. However, it must be kept in mind that the resin is a much more concentrated and het-

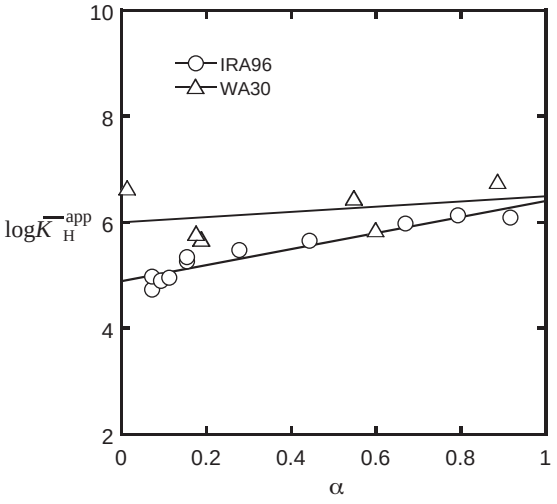


**Fig. 4.** The $p\bar{K}_a^{app}$ *vs.* $\alpha$ plots for the styrene–DVB-based weak base anion-exchange resins.

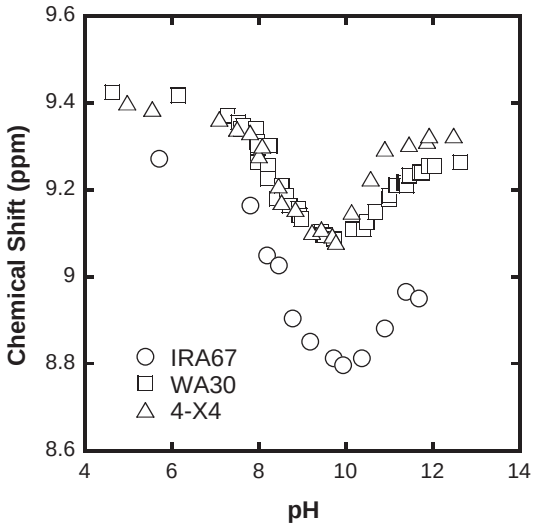


**Fig. 5.** The pH dependence of the $^{31}$P NMR chemical shifts of the phosphinate ion adsorbed into the acrylic acid–DVB-based weak base anion-exchange resins.

erogeneous solution, which can bring a different protonation or complexation behavior. The evaluated protonation constants of the styrene–DVB-based weak base anion-exchange resins were different from the protonation constant of *N*,*N*-dimethylbenzylamine: $\log K_H = 8.40$ [30]. Judging from the broad and asymmetric $^{31}$P signals of phosphinate ion in the resin phases, heterogeneity in distribution and/or structure of the tertiary amine groups introduced into the resins might be the reason for the difference. Anyway, it needs further consideration.

### 3.3. Acrylic acid–DVB-based resins

An acrylic-type weak base anion-exchange resin can be produced by introducing tertiary amine groups into the copolymers of acrylic acid and DVB. Amberlite IRA67, DIAION WA10 and Bio-Rad AG 4-X4 are commercially available acrylic acid–DVB-based weak base anion-exchange resins. The protonation equilibrium of the tertiary amine moiety of the resins can be written as follows:

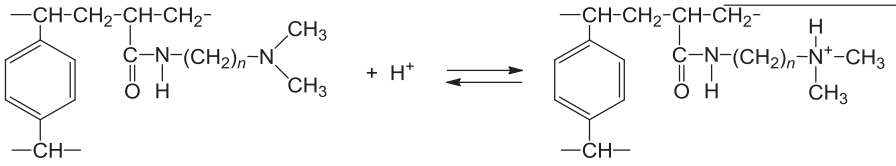


(9)

The pH dependence of the $^{31}$P NMR chemical shifts of the phosphinate ion adsorbed into the acrylic resins is shown in Fig. 5. In the same way as those for the styrene–DVB-based resins, the phosphinate signals shifted to the lower field at a lower pH in the range of 6–10 due to the protonation of the tertiary amine group. In addition to this low field shift, the signals for the acrylic resins shifted to a lower field even at a pH higher than 10, indicating that an unexpected acid dissociation might occur at this pH. Fig. 6 shows the $^{31}$P NMR signal intensity ratios of the phosphinate ion in the resin to that in the interstitial equilibrium solution at various pHs. As can be seen from the figure, the phosphinate ion was little present at a pH higher than 10, because the anion should be excluded from the resin phase probably due to the fixed minus charges produced at the high pH. In order to obtain complementary information about the ionic states of the fixed groups in the acrylic acid–DVB-based resins at a high pH, the $^{133}$Cs NMR spectra for the resins in equilibrium with the CsCl solutions of different pHs were recorded. Fig. 7(a) shows a $^{133}$Cs NMR spectrum for DIAION WA10 in equilibrium with a 0.1 mol dm$^{-3}$ CsCl solution at pH 10.4; the lower field signal was assigned to $Cs^+$ in the resin phase and the other to that in the equilibrium solution. The resin phase signal was asymmetric, reflecting the heterogeneity in the resin phase. The $^{133}$Cs NMR signal intensity ratio of $Cs^+$ in the resin phase to that in the interstitial equilibrium solution increased with an increase in the pH (Fig. 6), showing that the cation could appreciably get into the anion-exchange resin at a pH higher than 9. Taking into account the structures of the acrylic resins, the fixed minus charges would be produced in the functional group through a tautomerism accompanying the proton release from the amide form to the imide one, which produced the cation exchange ability of the weak base anion-exchange resin at the high pH. The tautomerism can be described as follows:

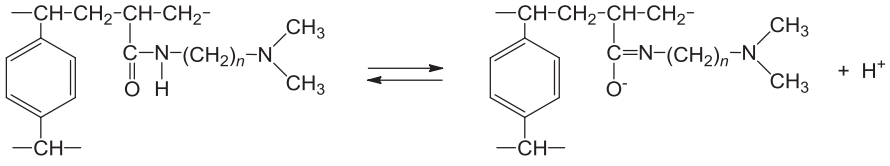


(10)

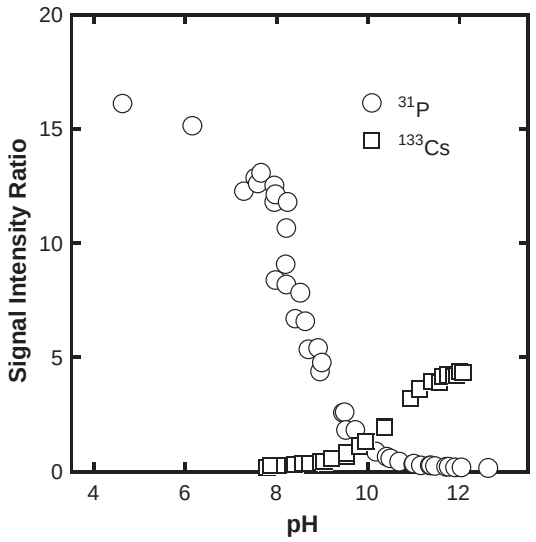


**Fig. 6.** The $^{31}$P and $^{133}$Cs signal intensity ratios for the ionic species in the DIAION WA10 resin to that in the equilibrium solution at various pHs. The NMR samples are the resins in equilibrium with 0.1 mol dm$^{-3}$ $NaPH_2O_2$ solutions for $^{31}$P and 0.1 mol dm$^{-3}$ CsCl solutions for $^{133}$Cs.

$$\bar{K}_a = \frac{\bar{a}_{R^-} \cdot \bar{a}_H}{\bar{a}_R} \tag{11}$$

Thus, the pH-dependent chemical shifts are given by the following equation:

$$\bar{\delta}_P = \frac{\bar{\delta}_P^{RH^+} \bar{K}_H \bar{a}_H + \bar{\delta}_P^{R} + \bar{\delta}_P^{R^-} \bar{K}_a / \bar{a}_H}{\bar{K}_H \bar{a}_H + 1 + \bar{K}_a / \bar{a}_H} \tag{12}$$

where $RH^+$, R and $R^-$ refer to the ionic states of the functional groups, that is, the protonated tertiary amine, unprotonated amine and deprotonated imide, and $\bar{\delta}_P^{RH^+}$, $\bar{\delta}_P^{R}$ and $\bar{\delta}_P^{R^-}$ are the $^{31}$P NMR chemical shifts of the phosphinate ion in the anion-exchange resins for each ionic state, respectively.

Due to the tautomerism accompanying the proton release, the $\log(\bar{a}_{PH_2O_2^-}/a_{PH_2O_2^-})$ values for the acrylic resins would decrease and not approach zero at a rather high pH, thus the conventional extrapolating method [27–29] to determine the thermodynamic protonation constants is not applicable for the acrylic resin systems. In order to evaluate the protonation constants, therefore, the activity of hydrogen ion in the acrylic resin phase should be estimated. The $^1$H NMR spectra were recorded for the same resin samples as those used for the already mentioned $^{133}$Cs NMR measurements (Fig. 7(b)). Two well-resolved signals were observed; the lower field signal was assigned to water in the resin phase and the other to that in the interstitial equilibrium solution. By assuming that the molar volume of water in the resin phase was equal to that in the equilibrium solution, we estimated the volume ratio ($\bar{V}/V$) of the resin phase to the interstitial solution in an NMR sample tube from the $^1$H NMR signal intensity ratios of water, and the $[\overline{Cs^+}]/[Cs^+]$ values were then calculated using the following equation:

$$\frac{[\overline{Cs^+}]}{[Cs^+]} = \frac{\bar{A}_{Cs}}{A_{Cs}} \frac{V}{\bar{V}} \tag{13}$$

where $A_{Cs}$ refers to the $^{133}$Cs signal intensity. By applying Donnan's theory to the $Cs^+/H^+$ ion exchange system, the activity of hydrogen ion in the resin phase was given as follows:

$$\bar{a}_H = a_H \frac{[\overline{Cs^+}]\bar{\gamma}_{Cs}}{[Cs^+]\gamma_{Cs}} \tag{14}$$

The activity coefficient of $Cs^+$ in the resin phase cannot be evaluated from the simple Gibbs–Donnan model, but it can be constant at a constant ionic strength. In this study the activity of hydrogen ion in the resin phase was estimated from Eq. (14) by assuming $\bar{\gamma}_{Cs}/\gamma_{Cs} = 1$. Fig. 8 shows the relationship of pH between DIAION WA10 and its equilibrium solution. The estimated pH in the resin phase is higher than that in the equilibrium solution below pH 9.5 and the resin acts as an anion-exchanger. Above this pH, on the other hand, the pH is lower in the resin phase and the resin acts as a cation-exchanger. The quantitative treatment of the acid dissociation related to the tautomerism accompanying the proton release was not considered further in this study, because of the difficulty in accurate pH measurements under the strongly basic conditions.

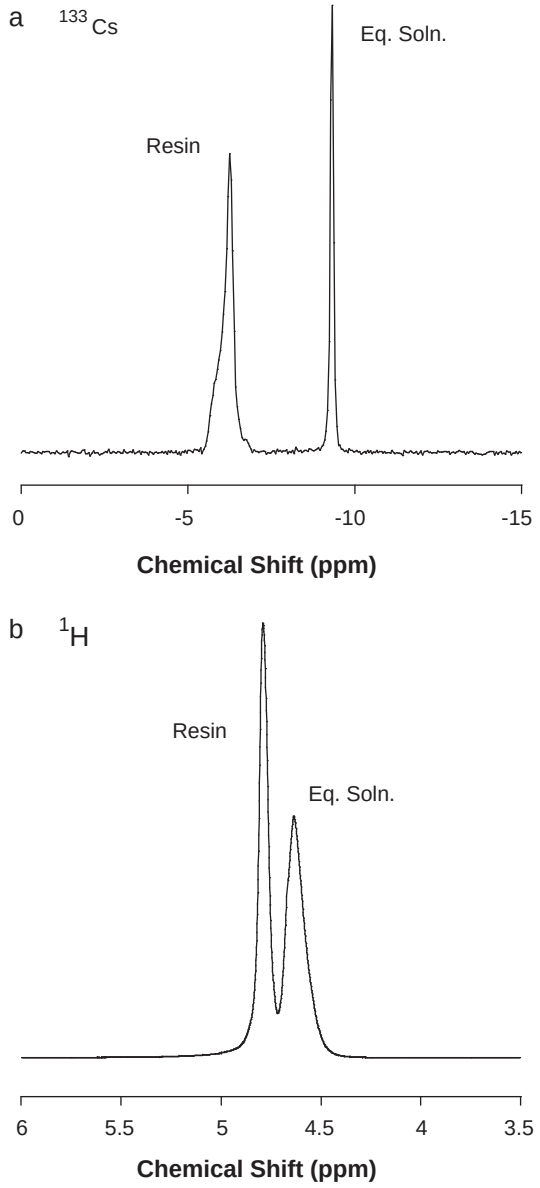


**Fig. 7.** The $^{133}$Cs and $^1$H NMR spectra for DIAION WA10 in equilibrium with a 0.1 mol dm$^{-3}$ CsCl solution at pH 10.4.

Under the pH condition when the tautomerism is ignored, we can obtain the following Henderson–Hasselbalch equation for the $^{31}$P chemical shift data from Eq. (12).

$$p\bar{H} = \log \bar{K}_H + \log \frac{\bar{\delta}_P - \bar{\delta}_P^{RH^+}}{\bar{\delta}_P^{R} - \bar{\delta}_P} \tag{15}$$

The values of $\bar{\delta}_P^{RH^+}$ and $\bar{\delta}_P^{R}$ were obtained from limiting values of a smooth curve fitted to the experimental data under the pH

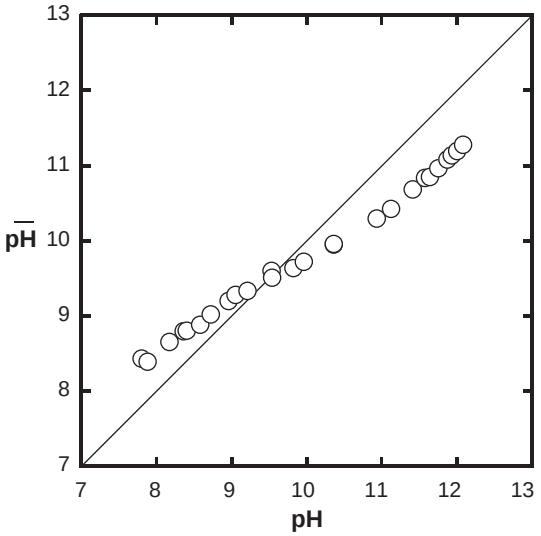


**Fig. 8.** Relationship of pH between the DIAION WA10 resin phase and its equilibrium solution.

condition when the tautomerism could be ignored. We can also obtain the same type of Henderson–Hasselbalch equation for the $^{31}$P signal intensity data as follows:

$$p\bar{H} = \log\ \bar{K}_H + \log\frac{R_P - R_P^{RH^+}}{R_P^R - R_P} \quad (16)$$

where $R_P^{RH^+}$ and $R_P^R$ are the signal intensity ratios of phosphinate ions in the resins with protonated or unprotonated functional groups to those in the equilibrium solutions, respectively. Since the value of $[\overline{Cs^+}]/[Cs^+]$ in Eq. (13) could nearly be one in the resins for unprotonated amine form, $R_P^R$ was supposed to be $\bar{V}/V$ which was estimated from the $^1$H NMR signal intensity ratio. The value of $R_P^{RH^+}$ was obtained from the lower pH limiting value of a smooth curve fitted to the experimental points in Fig. 6. Fig. 9(a) and (b) show the plots of $p\bar{H}$ *vs.* $\log(\bar{\delta}_P - \bar{\delta}_P^{RH^+})/(\bar{\delta}_P^R - \bar{\delta}_P)$ or $\log(R_P - R_P^{RH^+})/(R_P^R - R_P)$ for DIAION WA10. Good linear relationships were obtained and the protonation constant of the tertiary amine moiety of DIAION WA10 was obtained to be $\log \bar{K}_H = 8.8 \pm 0.1$ and $8.9 \pm 0.1$ from the *y*-intercept values of the plots of Eq. (15) and (16), respectively. The protonation constants of the tertiary amine moieties were $\log \bar{K}_H = 9.0 \pm 0.1$ (from the chemical shift data) and $9.2 \pm 0.4$ (from the signal intensity data) for Amberlite IRA67, and $9.3 \pm 0.1$ (from the chemical shift data) and $9.1 \pm 0.3$ (from the signal intensity data) for Bio-Rad AG 4-X4. These values are compared with the protonation constants of *N*,*N*-dimethylbenzylamine ($\log K_H = 8.40$ [30]) and trimethylamine ($\log K_H = 9.80$ [31]) in aqueous solutions. The difference of the protonation constants between the acrylic acid–DVB-based resins and the monomeric models in aqueous solutions might be partly ascribed to the activity coefficient ratio $\bar{\gamma}_{Cs}/\gamma_{Cs}$. While the activity coefficients in the resin phases were not estimated in this study, the values of $\bar{\gamma}_{Cs}/\gamma_{Cs}$ should be closed to unity, because the differences were not very high.

The quantitative analysis of NMR signal intensity ratios of the species between the resin phase and the equilibrium solution was possible, if the resins could be packed into NMR sample tubes with an identical and uniform packing state for every resin bed sample as in the case for the gel type resins: IRA67 and WA10, or the grinded macroporous resin: 4-X4. In the case of IRA96 and WA30, however, it was difficult to pack the macroporous resin beads identically and uniformly. Moreover, the $^1$H signals of water in the styrene–DVB-based resins and that in the interstitial equilibrium solutions were observed at the same positions, so that the values of $[\overline{Cs^+}]/[Cs^+]$, and then, the activities of hydrogen ion in the resin phases could not be estimated. For these reasons, the protonation constants of the styrene–DVB-based resins were not evaluated by the method applied to the acrylic acid–DVB-based resins.

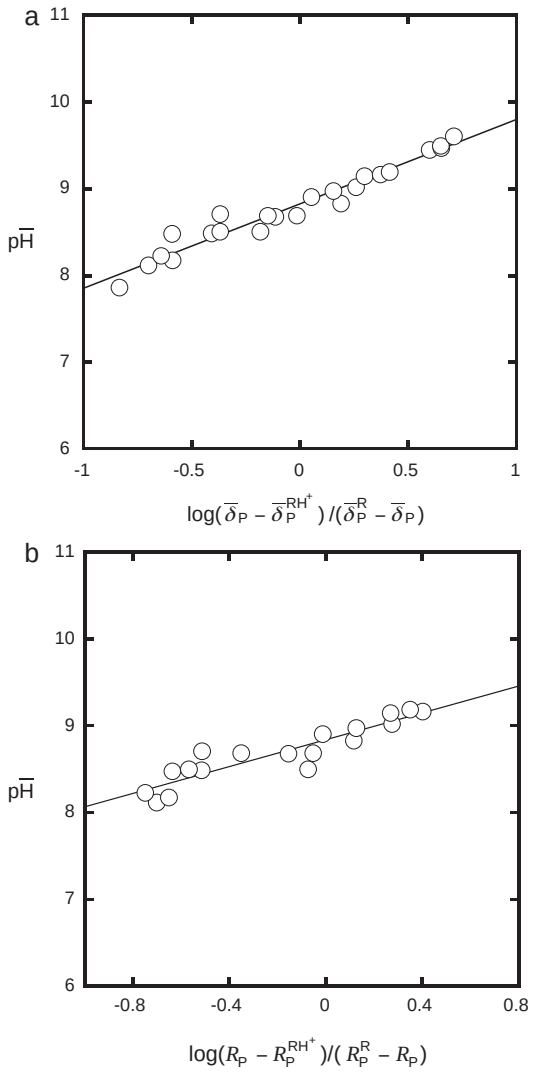


**Fig. 9.** The plots of Henderson–Hasselbalch equations (a) Eq. (15) and (b) Eq. (16) for DIAION WA10.

## 4. Conclusion

Protonation behaviors of styrene–DVB based and acrylic acid–DVB based weak base anion-exchange resins, in which tertiary amine moieties were introduced as a functional group, were clarified on the basis of the information about the solution environment of the resin internal phases acquired by the original NMR technique probing the species adsorbed into the resins. The data obtained by the NMR method also revealed that the acrylic-type weak base anion-exchange resins could produce protons through the tautomerism of the functional group from the amide form to the imide one at high pH. As a result of this acid dissociation, the acrylic resins could unexpectedly act as cation-exchangers. The NMR spectroscopy of the species in the resin phase allowed a new insight into the practical use of weak base anion-exchange resins as well as detailed information about the equilibria taking place inside the resins.

## Acknowledgements

We thank the Mitsubishi Chemical Corporation and Nippon Rensui Corporation for their kind donation of the DIAION ion-exchange resins, and the Organo Corporation for the Amberlite ion-exchange resins.

## References

[1] K. Dorfner (Ed.), Ion Exchangers, Walter de Gruyter, Berlin/New York, 1991.
[2] H.F. Walton, R.D. Rocklin, Ion Exchange in Analytical Chemistry , CRC Press, Inc., Boca Raton/Ann Arbor/Boston, 1990.
[3] F. Helfferich, Ion Exchange , McGraw-Hill, New York, 1962.
[4] Y. Marcus, A.S. Kertes, Ion Exchange and Solvent Extraction of Metal Complexes , Wiley-Interscience, London, 1964.
[5] E. Högfeldt, React. Polym. 11 (1989) 199.
[6] W.H. Höll, J. Horst, M. Wernet, React. Polym. 14 (1991) 251.
[7] Ö. Szabadka, Talanta 29 (1982) 183.
[8] Y. Merle, J. Marinsky, Talanta 29 (1984) 199.
[9] J. Marinsky, T. Miyajima, E. Högfeldt, M. Muhammed, React. Polym. 11 (1989) 279.
[10] M. Pesavento, A. Profumo, R. Biesuz, React. Polym. 11 (1989) 37.
[11] M. Pesavento, R. Biesuz, M. Gallorini, A. Profumo, Anal. Chem. 65 (1993) 2522.
[12] M. Pesavento, R. Biesuz, React. Funct. Polym. 36 (1998) 135.
[13] R. Biesuz, G. Alberti, M. Pesavento, J. Solution Chem. 37 (2008) 527.
[14] M. Busch, E.V. Boldammer, J. Solution Chem. 11 (1982) 777.
[15] T. Zawodzinski, M. Neeman, L. Sillerud, O. Gottesfeld, J. Phys. Chem. 95 (1991) 6040.
[16] D. Reichenberg, I.J. Lawrenson, Trans. Faraday Soc. 59 (1963) 141.
[17] Y. Miyazaki, H. Waki, J. Chem. Soc., Faraday Trans. 89 (1993) 3925.
[18] Y. Miyazaki, G. Kura, H. Tsuzuki, H. Sakashita, J. Chem. Soc., Faraday Trans. 92 (1996) 3587.
[19] G. Kura, Y. Miyazaki, H. Waki, A. Marton, React. Funct. Polym. 38 (1998) 197.
[20] A. Marton, Y. Miyazaki, Prog. Colloid Polym. Sci. 117 (2001) 153.
[21] A. Marton, H. Sakashita, Y. Miura, E. Hiramatsu, Y. Miyazaki, Talanta 59 (2003) 217.
[22] Y. Miyazaki, H. Qu, J. Konaka, Anal. Sci. 24 (2008) 1123.
[23] K. Yoshimura, Y. Miyazaki, F. Ota, S. Matsuoka, H. Sakashita, J. Chem. Soc., Faraday Trans. 94 (1998) 683.
[24] G. Szentes, A. Marton, Y. Miyazaki, J. Ion Exch. 14 (Suppl.) (2003) 29.
[25] E. Högfeldt (Ed.), Stability Constants of Metal–Ion Complexes. Part A. Inorganic Ligands, Pergamon Press, Oxford/New York/Toronto/Sydney/Paris/Frankfurt, 1982, p. 130.
[26] R.M. Smith, A.E. Martell (Eds.), Critical Stability Constants, vol. 6, 2nd Suppl., Plenum Press, New York/London, 1989, p. 204.
[27] T. Miyajima, in: J.A. Marinsky, Y. Marcus (Eds.), Ion Exchange and Solvent Extraction, vol. 12, Marcel Dekker, Inc., New York/Basel/Hong Kong, 1995, p. 275.
[28] R. Biesuz, A.A. Zagorodni, M. Muhammed, J. Phys. Chem. B 105 (2000) 4721.
[29] C. Rey-Castro, R. Herreo, M.E. Sastre de Vincente, J. Electroanal. Chem. 564 (2004) 223.
[30] J. Armstrong, R.B. Barow, Br. J. Pharm. 57 (1976) 501.
[31] A.E. Martell, R.M. Smith (Eds.), Critical Stability Constants, vol. 5, 1st Suppl., Plenum Press, New York/London, 1982, p. 435.